

# Synthesis and Characterization of Cerium Oxide Nanoparticles using *Curvularia lunata* and Their Antibacterial properties

S.Munusamy<sup>1</sup>, K. Bhagyaraj<sup>1</sup>, L.Vijayalakshmi<sup>3</sup>, A. Stephen<sup>2</sup>, and V.Narayanan<sup>1\*</sup>

<sup>1</sup>Department of Nuclear Physics, Guindy Campus, University of Madras, Chennai – 600025, India

<sup>2</sup>Department of Inorganic Chemistry, Guindy Campus, University of Madras, Chennai – 600025, India

<sup>3</sup>TMG College of Arts and Science<sup>4</sup>, Manimangalam, Chennai-601301, India

Corresponding author -vnnara@yahoo.co.in

**Abstract-** In the present work, we have investigated synthesis of cerium oxide nanoparticles (CeO<sub>2</sub> NPs) using *Curvularia lunata* culture filtrate. The synthesized CeO<sub>2</sub> NPs were characterized by TG/DTA, XRD, Raman, PL, FTIR, UV-visible spectroscopy and TEM analyses. The synthesized nanoparticles retained the cubic structure, which was confirmed by X-ray diffraction studies. UV-visible spectrum exhibited a well defined absorption peak at 298.35 nm. TEM images showed that the NPs possessed spherical shape and particle size range from 5 to 20 nm. Application of the synthesized CeO<sub>2</sub> NPs was investigated by antibacterial activity, which shows a significant inhibition towards both gram positive and gram negative bacteria.

**Keywords-** *Curvularia lunata*, CeO<sub>2</sub> NPs, Raman spectroscopy, TEM, Antibacterial activity

## I. INTRODUCTION

Nanotechnology has varied applications in lifestyle. Surface to the volume ratio is the high impact of nanoparticles (NPs), and it's containing lot of physical and chemical properties. Cerium oxide (CeO<sub>2</sub>) is a semiconductor with wide band gap energy (3.19eV) and large exciton binding energy [1]. It is used for wide range of applications like electronics [2], bio-sensors [3], drug delivery [4], agriculture [5], pharmaceutical and medical [6]. Generally CeO<sub>2</sub> NPs can be synthesized by physical, chemical and green methods [7-15]. Nowadays, mycosynthesis method is more advantages as well as handled with easy process, cost effectiveness, energy and time consume technique [16]. The fungal extracellular compounds such as enzymes, proteins and hetero - cyclic derivatives, which act as quit promising fellow for reducing and capping agent for good bio catalytic performance [17-20]. The past two decades, many researchers focused on transition metal nanoparticles. Very few works has been done in the metal oxide nanoparticles synthesis. Until now, only one attempt was found to the CeO<sub>2</sub> NPs were synthesized by *Humicola* sp culture filtrate [21]. However, mycosynthesized CeO<sub>2</sub> NPs have more stability, water dispersible, high fluorescent properties and did not agglomerate[21-23]. So, we attempted in the synthesized CeO<sub>2</sub> NPs using *C. lunata* culture filtrate. In the present investigation, synthesis and characterization of CeO<sub>2</sub> NPs using *C. lunata* culture filtrate and their potential applications for antibacterial activity is discussed. To the best of our knowledge, this is the first report on the mycosynthesis of CeO<sub>2</sub> NPs were nontoxic and high yield for large scale. It can be an alternative for the improvement of the drugs for human diseases.

## II. EXPERIMENTAL

### A. Materials

#### Chemicals

Cerium (III) chloride heptahydrate (CeCl<sub>3</sub>·7H<sub>2</sub>O) was obtained from Merck. Microbiological media were obtained from Himedia laboratories, India. Double distilled water, analytical grade chemical and reagents were used for all the experiments.

#### Identification of fungus

The *C. lunata* culture was collected from PG and Research Department of Plant Biology and Plant Biotechnology, Ramakrishna Mission Vivekananda College, Chennai. The identified fungus *C. lunata* have small size of micro conidia, characterized using light microscope (Euromex, model: GE3045, the Netherlands) at a magnification of 40X.

### Inoculation

*C. lunata* spores were aseptically inoculated in the Czapek-Dox-Broth (CDB) medium containing 30 g sucrose, 3 g sodium nitrate, 1 g dipotassium hydrogen phosphate, 0.5 g magnesium sulfate and 0.01 g ferrous sulfate, pH was adjusted to 6.5 with 0.1 N NaOH or 0.1 N HCl before autoclave at 121°C and 15 lb for 20 min.

### B. synthesis of cerium oxide nanoparticles

*C. lunata* was inoculated in Czapek-Dox- Broth (CDB) medium. The conical flask containing medium was incubated at 37°C and agitated at 120 rpm for 72 h. After the incubation, the fungus spores produced black color mycelium in the medium. The fungal mycelium contain culture medium filtered through Whatman filter paper No.1. and the filtrate was collected in 250 ml Erlenmeyer flask and stored at room temperature for further usage. Thereafter, 3.72 g  $\text{CeCl}_3 \cdot 7\text{H}_2\text{O}$  salt was added to 100 ml of fungal culture filtrate. This solution was stirred constantly at a temperature of 80 °C for 4-6 h. A white precipitate formed and then it became a yellowish brown in color on continuous stirring. Further the precipitate was calcined at 350 and 400 °C for 2 h. Thus,  $\text{CeO}_2$  nanopowder was obtained.

### C. Characterization methods

The XRD pattern was recorded using Cu K radiation ( $\lambda = 1.54060 \text{ \AA}$ ) with nickel monochromator in the range of  $2\theta$  from  $10^\circ$  to  $80^\circ$ . The average crystallite size of the synthesized  $\text{CeO}_2$  NPs was calculated using Scherrer's formula [ $D = 0.9 \lambda / \cos \theta$ ]. The Micro Raman analysis of our samples carried out using Princeton Acton SP2500, CS spectrometer, 0.5 Focal length triple grating monochromator, excitation source  $\text{Ar}^+$  laser, 514.5 nm wavelength. Photoluminescence measurement was carried out on a luminescence spectrophotometer (Perkin Elmer LS-5513, Perkin Elmer Instrument, USA) using xenon lamp as the excitation source at room temperature. Fourier transform infrared spectroscopy (FTIR) analysis was carried out in the range of 400-4000  $\text{cm}^{-1}$ . UV- visible spectroscopy in the wavelength range of 200-850 nm using Perkin Elmer spectrophotometer,. The morphology of the synthesized  $\text{CeO}_2$  was examined using TEM.

### D. Antibacterial activity of $\text{CeO}_2$ NPs

The antibacterial activity of the synthesized  $\text{CeO}_2$  NPs were examined under three Gram positive (G<sup>+</sup>) (*Staphylococcus aureus*, *Streptococcus pneumoniae* and *Bacillus subtilis*) and three Gram negative (G<sup>-</sup>) bacteria (*Pseudomonas aeruginosa*, *Proteus vulgaris* and *Klebsiella pneumoniae*) by disc diffusion method [24]. These six bacterial strains were grown in nutrient broth at 37 °C until the bacterial suspension reached  $1.5 \times 10^8$  CFU/mL. Approximately 20 mL of molten nutrient agar was poured into the Petri dishes and cooled. All the bacterial suspension was swapped over the medium, the disc loaded in three different concentrations 10, 50 and 100 mg of  $\text{CeO}_2$  NPs using sterile distilled water and they were placed over the medium using sterile forceps. The plates were then incubated for 24 h at 37 °C. The inhibition zone formed around each discs were measured. Each experiment was conducted in triplicate.

## III.RESULTS AND DISCUSSION

### A. XRD analysis

X-ray diffraction pattern was recorded for the as synthesized material, material calcined at 350 and 400oC. The as synthesized and 350oC calcined material did not show any clear intense peaks, which is due to the amorphous state. In addition, the 400oC calcined sample exhibited four diffraction peaks at 28.49o, 33.01o, 47.42o and 56.28o respectively indexed with (1 1 1), (2 0 0), (2 2 0) and (3 1 1) planes for the cubic fluorite structure of  $\text{CeO}_2$  in the standard data (JCPDS card no: 89-8436) [Figure.1]. It is clearly seen that the diffraction peaks become sharper and narrower with increasing calcination temperature. The low intense peaks at 59.01o, 69.34o, 76.66o and 79.17o belongs to (2 2 2), (4 0 0), (3 3 1) and (4 2 0) planes. Using the Scherrer formula the average size of the particle was estimated to be around 5 nm [20].

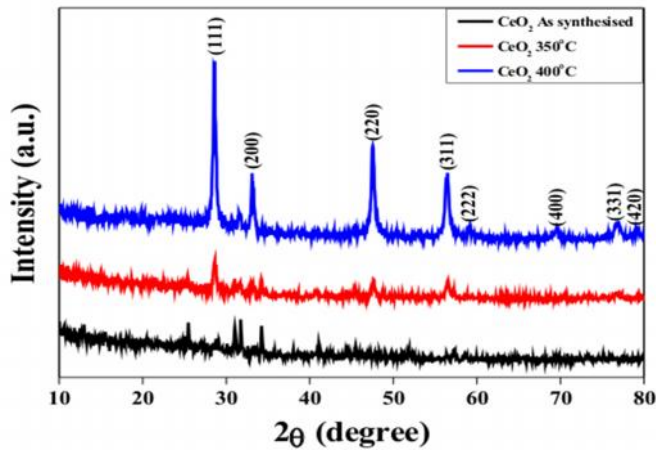


Figure.1. XRD analysis of mycosynthesized CeO<sub>2</sub> NPs

B. Micro Raman and PL analysis

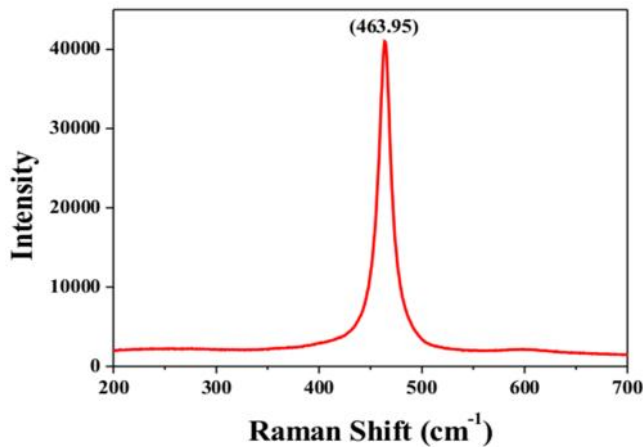


Figure.2 Raman spectrum of mycosynthesized CeO<sub>2</sub> NPs

synthesized CeO<sub>2</sub> NPs was further elucidated by using Micro Raman spectroscopy. The Raman spectrum exhibited a strong intense band at 463.95 cm<sup>-1</sup> [Figure.2]. The Raman active mode is attributed to a symmetrical stretching mode of the CeO<sub>2</sub>. It generally corresponds to the F<sub>2g</sub> Raman active mode of fluorite cubic structure [15]. Room temperature PL spectrum of the CeO<sub>2</sub> NPs sample measured using xenon laser of 290 nm. The spectra of the CeO<sub>2</sub> sample mainly consist of six emission peaks: The weak blue bands at 363 and 378 nm, a broad emission band at 395 nm, a weak blue band at 413 nm, again a blue band at 459 nm and weak blue green band at 492 nm. The dependence of PL blue-shift peak on CeO<sub>2</sub> particle concentration has also been observed. This phenomenon has been explained by charge transition from the 4f band to the valance band of the CeO<sub>2</sub> NPs. In this sample, the weak blue and weak blue- green emissions are possibly due to surface defects in the CeO<sub>2</sub> NPs, and the low intensity of the green emission peak due to the low density of oxygen vacancies during the preparation of the sample. Broad peak centered at 395 nm for the CeO<sub>2</sub> sample calcined at 400°C originate from the defect states existing between the Ce 4f state and O 2p valance band [15].

C. UV-visible spectroscopy

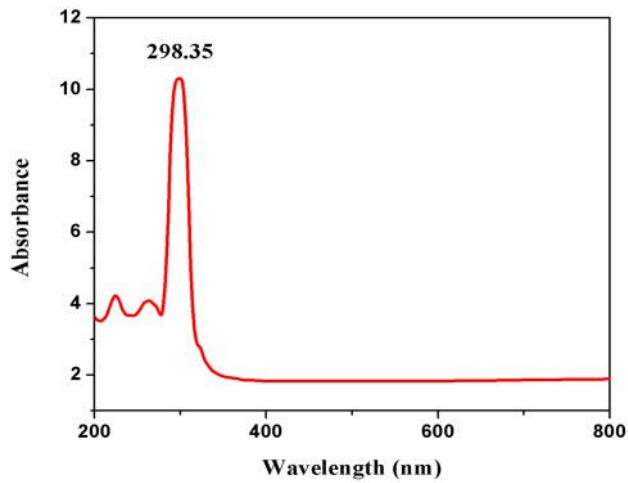


Figure.3 UV- visible spectrum of mycosynthesized CeO<sub>2</sub> NPs

synthesized CeO<sub>2</sub> NPs in water sample was subjected to UV-visible spectroscopy analysis exhibited a well defined absorption peak at 298.35 nm [Figure.3], which shows the CeO<sub>2</sub> NPs having a better optical property. Usually the peak at 298 nm corresponds to the fluorite cubic structure of CeO<sub>2</sub> NPs, due to the quantum size effect of the blue shift in the UV-visible spectra and confirm that charge between the O 2p and Ce 4f states in O<sup>2-</sup> and Ce<sup>4+</sup>[3,14].

D. TEM analysis

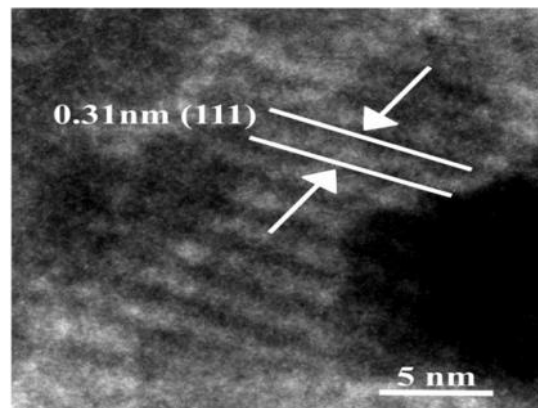


Figure- 4. TEM image of mycosynthesized CeO<sub>2</sub> NPs

The morphology and structure of the powders were investigated by TEM. The images with corresponding selected-area electron diffraction (SAED) patterns and high resolution TEM images of the CeO<sub>2</sub> sample. It can be seen that the synthesized CeO<sub>2</sub> sample contains agglomerated particles with particle size 5 nm [Figure.4]. The SAED pattern of CeO<sub>2</sub> sample resulted the characteristics ring pattern of fluorite cubic structure and they infer the higher degree of crystallinity of CeO<sub>2</sub> NPs [25].

E. Antibacterial activity

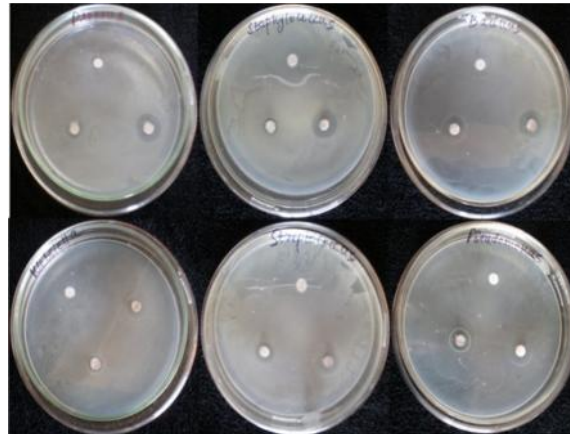


Figure.5 Antibacterial activity of mycosynthesized CeO<sub>2</sub> NPs

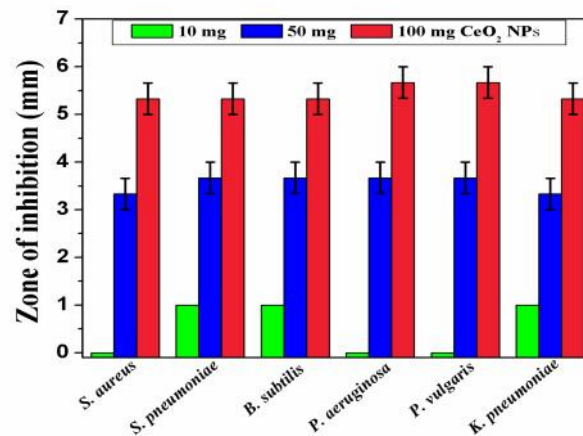


Figure.6 Antibacterial activity of mycosynthesized CeO<sub>2</sub> NPs at different concentrations on Gram positive and negative bacterial strains .

The antibacterial activity was performed against three Gram positive and Gram negative bacterial pathogens using three different concentrations 10, 50 and 100 mg of CeO<sub>2</sub> NPs. In 50 mg concentration CeO<sub>2</sub> NPs showed a most significant effect on zone of inhibition in  $3.67 \pm 0.33$  mm of *S. pneumoniae*, *B. subtilis*, *P. aeruginosa* and *P. vulgaris*. The *S. aureus* and *K. Pneumoniae* exhibited a modulated effect on inhibition zone in  $3.33 \pm 0.33$  mm. In addition, 100 mg concentration showed higher activity on zone of inhibition in  $5.67 \pm 0.33$  of *P. aeruginosa* and *P. vulgaris*. The *S. aureus*, *S. pneumoniae*, *B. subtilis*, and *K. Pneumoniae* clearly showed average zone of inhibition at  $5.33 \pm 0.33$ . So for, 100 mg concentration of CeO<sub>2</sub> NPs has better antibacterial activity when compared to 10 and 50 mg concentration [Figure.5-6]. Generally, antibacterial activity of metal and metal oxide nanoparticles is due to the interaction of nanoparticles on to the bacterial cell wall by electrostatic attraction between the negatively charged bacteria and positively charged nanoparticles. In this interaction not only inhibit the bacterial growth and induce the reactive oxygen species (ROS) generation, which leads to cell death [26]. The actual mechanism of antibacterial activity of CeO<sub>2</sub> NPs takes place on the interfere with the bacteria cell membrane and binding with mesosome will there by disturb the mesosomal functions of cellular respiration, DNA replication, cell division and increased the surface area of bacterial cell membrane these intracellular functional changes of oxidative stress induced by ROS generation due to the cell expiry.

#### IV. CONCLUSION

In summary, CeO<sub>2</sub> NPs have been successfully synthesized using *C. lunata* culture filtrate. The XRD patterns, Micro Raman spectra and SAED pattern studies suggest the formation CeO<sub>2</sub> NPs cubic fluorite structure. The TEM images clearly showed spherical morphology with the average size of 5 nm. synthesized CeO<sub>2</sub> NPs were investigated by antibacterial activity. The perusal results observed at 100 micro gram CeO<sub>2</sub> NPs had most significant effect of antibacterial activity due to the strong electrostatic forces to binding the bacterial cell membrane to inhibit the bacterial growth. We believe that a simple, reliable, cost effective and eco-friendly method using fungal extracellular compounds can be extended to the synthesis of other metal and metal oxide NPs.

#### ACKNOWLEDGEMENT

The authors gratefully thank full UGC-CPEPA financial supports university of madras and National Center for Nanoscience for extending the TEM image facility.

#### REFERENCES

- [1] Miao, J.J. Wang, H. Li, Y.R. Zhu, J.M. Zhu, J.J. J. Cryst. Growth, No. 281 pp. 525-529,2005
- [2]. Yahiro, H., Baba, Y., Eguchi, K., Hiromichi A., J. Electrochem. Soc.No. 135 pp. 2077-2080,1998
- [3] Khan, S.B., Faisal, M., Rahman, M.M., and. Jamal, Sci. Total Environ.No. 409 pp.2987-2992, 2011.
- [4] Patil, S., Sandberg A., Heckert E. Self., W S., Seal, BiomaterialsNo. 28 pp. 4600-4607,2007
- [5] Zhang P.,Ma Y., Zhang, Z., He, X., Zhang, J., Guo, Z., Tai, R., Zhao, Y., Chai, Z., ACS Nano No. 11 pp.9943-9950. 2012
- [6] O Thill., Zeyons Spalla, O., Chauvat,,F., Rose, J. Auffan,M., Flank, A. M., Environ. Sci Technol. No.40 pp.6151-6156. 2006
- [7]. Zhang, F., Chan, S. W., Spanier, J.E., Apak, E., Q. Jin, R.D. Robinson, I.P. Herman, Appl. Phys. Lett. No.80 pp.127-129, 2002
- [8] Hu, J, Li, Y. Zhou, X., Cai, M., Mater. Lett. No.61 (2007) pp.4989-4992.
- [9]H. Wang, J.J. Zhu, J.M. Zhu, X.H. Liao, S. Xu, T. Ding, H.Y. Chen, Phys. Chem. Chem. Phys.,No.4 pp. 3794-3799,2002
- [10]. Liao, X.H., Zhu J.M., Zhu, J.J., Xu J.Z., Chem. Commun, pp. 937-938,2001
- [11] Czerwinski, F., Szpunar, J.A., J. Sol-Gel Sci. Technol. No.9 (1997) pp.103-114.
- [12] Yao, S.Y. Xie, Z.H. J. Mater. Process. Tech.No. 186 pp.54-59,2007
- [13] Darroudi, M. Hoseini, S.J. Oskuee, R.K. Hosseini, H.A. Gholami, L. Gerayli, Ceram. Int. No.40 pp.7425,2014
- [14] Maensiri, S. Masingboon, C, Laokul, W. Jareonboon, V. Cryst. Growth Des. No. 7 (2007) pp.950-955.
- [15]Maensiri, S. Labuayai, S. Laokul, J Klinkaewnarong., Swatsitang, E, Jpn. J. Appl. Phys.No. 53 pp.06-14,2014
- [16]Mohanpuria, P. Rana, N.K. Yadav, S.K. J. Nanopart. Res. No.10 (2008)pp. 507-517.
- [17]N. Soni, S. Prakash. J. Rep. Parasitol. No.2 (2012)pp. 1-7.
- [18]. Balaji, D.SBasavaraja, S., Deshpande, R., Bedre Mahesh, D., Prabhakar, B.K., A, Colloids Surf. B, No. 68)pp. 88-92,2009
- [19] Rajakumar, G. Abdul Rahuman A. Mohana Roopan, S, Gopiesh Khanna V., G. Elango, C. Kamaraj, A, Abduz Zahir. K. Velayutham, Spectrochim. Acta A, No 91 pp.23-29,2012
- [20] Gopinath, K., Arumugam, A., Appl. Nanosci. doi: 10.1007/s13204-013-0247-4.
- [21] Khana S.A. Ahamad A. Mater. Res. Bull. No.48. pp.4134-4138,2013
- [22] Bhainsa, K.C., D'Souza, S.F., Colloids Surf. B, No. 47) pp. 160-164,2006
- [23]. Gopal, J.V., Thenmozhi, M., Kannabiran, K., Rajakumar, G., Velayutham, K., Mater. Lett.No. 93 pp. 360-362,2013
- [24]. Gopinath K, Karthika V., Gowri S. Arumugam, A., J. Nanostruct. Chem. No.4) pp.83,2014
- [25] Phoka, S. Laokul P., Swatsitang E., Promarak, S., Maensiri, Mater. Chem. Phys. No.115 pp.423- 428,2009.